

# Simulation of Single Complex Macromolecules. 1. Structure and Dynamics of Catenanes

T. Pakula<sup>\*,†,‡</sup> and K. Jeszka<sup>‡</sup>

Max-Planck-Institute for Polymer Research, Postfach 3148, 55021 Mainz, Germany, and Institute of Polymers, Technical University of Lodz, Lodz, Poland

Received February 22, 1999; Revised Manuscript Received July 14, 1999

**ABSTRACT:** The cooperative motion algorithm is applied to simulate single macromolecules with complex topologies. Macromolecules of various topologies are represented by lattice structures corresponding to backbone skeletons of polymers. The structural and dynamic properties of chains of concatenated rings are analyzed as a function of two parameters: the ring size and the number of rings. Properties of the catenanes are compared with the behavior of simple linear and cyclic chains simulated under the same conditions.

## Introduction

This paper is the first of a series of publications that will present computer-simulated properties of single macromolecules with structures that cannot easily be synthesized by currently known methods. We have been motivated to undertake these studies by the fact that efforts of chemists to synthesize more complex molecules are often directed toward structures that are presumed to have new potentially interesting properties (e.g., refs 1 and 2). This, however, cannot be proven before a synthetic success. On the other hand, various complex molecular structures can easily be generated by a computer, and using appropriate simulation algorithms, their structure and dynamics can be studied under various external conditions.<sup>3–5</sup> We have in mind various nonlinear macromolecules, such as branched or hyperbranched polymers, dendrimers, stars, comb polymers, catenanes, and ladder- and platelike molecules as well as microgels. Only some of these structures have been previously studied by means of simulations.<sup>6–10</sup> Most attention has been devoted in the past to the behavior of linear polymers.

Besides various topologies, also various distributions of comonomers or functional groups within such molecules can influence their structure and properties (e.g., refs 11 and 12). This, however, is often even more difficult to control in the synthesis. Simulations of single macromolecules with a variation of topologies and variation of distributions of interacting elements will be considered in this series. It is expected that such studies will help to recognize structures with new interesting properties and in this way can help to direct synthetic efforts.

Experimental determination of details of behavior of single molecules constitutes also a big problem. There is a very limited number of experimental methods that are sensitive enough and have enough high resolution to be applicable for studies of single macromolecules. Therefore, also from this point of view, simulations should be considered as a valuable source of information about the behavior of single complex molecules.

A version of the cooperative motion algorithm (CMA)<sup>10,13</sup> is applied here to simulate single lattice polymers in which the most important features of the structure are taken into account. The molecules are represented by assemblies of beads (representing monomers) connected by nonbreakable bonds in a way corresponding to the skeleton of polymer chain backbones. Such molecular structures are organized on a lattice under the excluded-volume condition.

In this paper, we present results concerning catenanes, constituting a specific class of macromolecular architectures in which chemical bonds are to some extent replaced by topological connections between molecular elements. A synthesis of macromolecular systems consisting of concatenated rings has become a challenge for many synthetic chemists.<sup>1,14</sup> In spite of a lot of efforts, only a few systems have been synthesized that can be considered as belonging to this class of macromolecular structures.<sup>14–17</sup> Properties of catenanes will be compared with the behavior of linear and simple cyclic macromolecules.

## Polymer Models and Simulation Method

The architecture of complex polymers will be represented here by simplified models consisting of beads connected by nonbreakable bonds in a way corresponding to backbone contours of macromolecules. Such molecules will consist usually of a large number of beads assuming specific positions within a complex bond skeleton characteristic for each type of the macromolecule. This is a simplified representation of macromolecular structures in which sizes of monomers are not distinguishable. With this approximation, the macromolecules can, however, be represented on lattices. An example of such representation of a linear macromolecule on the face-centered-cubic (fcc) lattice is shown in Figure 1.

Macromolecules can be quite flexible rearranging all the time in space, preserving, however, the connectivity between beads given by the bond skeleton. To provide lattice molecules with sufficient flexibility, we apply concepts of bead rearrangements used previously in simulations of dense polymer systems on lattices.<sup>13</sup> The cooperative motion algorithm (CMA) has been described

<sup>†</sup> Max-Planck-Institute for Polymer Research.

<sup>‡</sup> Technical University of Lodz.

\* Corresponding author.

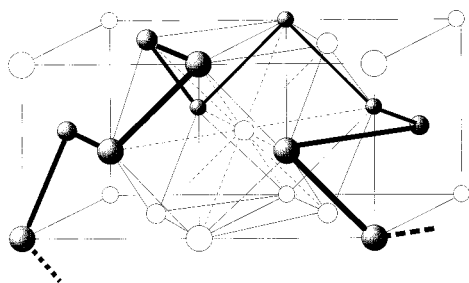


**Figure 1.** A representation of a linear macromolecule on the fcc lattice by means of beads connected by nonbreakable bonds.

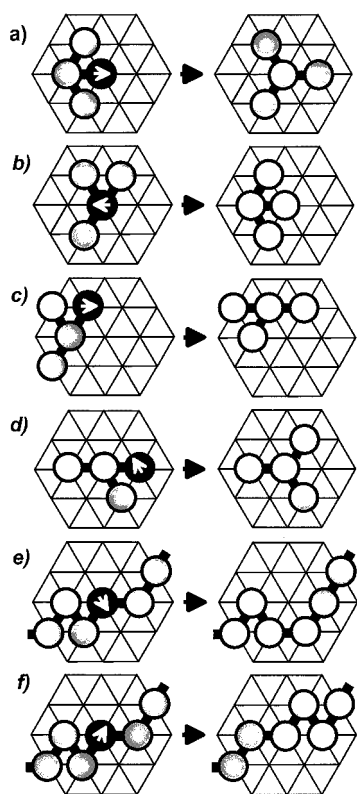


**Figure 2.** Examples of rearrangements of the molecule consisting of four beads on a triangular lattice (a–d) as well as typical local rearrangements within a fragment of a linear chain (e and f). Rearrangements result from motion attempts initiated from a randomly chosen atom (black) and directed as indicated by the arrow (white). Left- and right-hand side figures show states before and after rearrangements, respectively.

in several other publications [e.g., refs 5, 10, and 13] and is used here for single macromolecules. In this case, sequential attempts of rearrangements of bead groups are considered. A single attempt consists of several steps, including a random choice of a bead within the model macromolecule, a random choice of the direction of its attempted displacement, and a test of constraints given by bonds with neighbors as well as by the excluded-volume condition. Examples of moves resulting from successful attempts of this kind are illustrated in Figure 2 for some conformations of a simple branched four-bead molecule (a–d) as well as for an exemplary local conformation of a linear chain (e and f). It is assumed that the black bead is that which has been chosen randomly and that its motion direction is also random. The resulting rearrangements can involve displacements of one or more beads. The displacements of beads change the conformation of the molecule, but

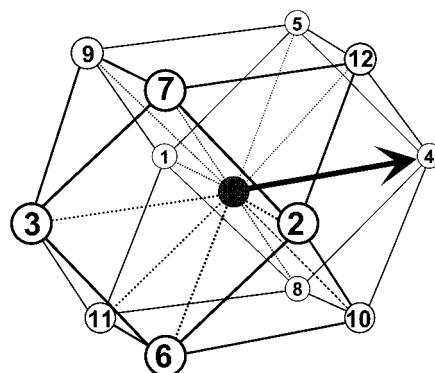


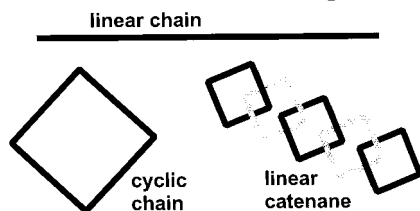
**Figure 3.** Coordination cell of the fcc lattice illustrating the orientation code of the site–site vectors.

its identity given by the specific architecture of the bond skeleton and positions of beads within the skeleton remains preserved. A large variety of rearrangements are possible, and therefore, we are not able to specify all of them.

The CMA is suitable for studies of static properties of macromolecular models as well as for characterization of their dynamic behavior in a broad time range.<sup>10</sup> Examples of rearrangements shown here are for the 2-dimensional case which is taken only for illustration. Simulations of various molecular objects which will be presented are performed for 3-dimensional systems on the fcc lattice. The lattice in all considered cases is used only as a coordination skeleton of the space. It helps to identify neighbors. Distances between lattice sites do not influence the rules of rearrangements in the athermal cases, as considered here.

In a model system, each bead is described by a sequence of numbers defining its position in the lattice, connectivity with other atoms in a molecule, and some of its properties:  $[m, i, j, k, a, c, \dots]$  where  $m$  is the index of the atom in a molecule,  $i, j$ , and  $k$  are indices of lattice sites along  $x, y$ , and  $z$  directions coinciding with axes of the fcc unit cell,  $a$  describes the bead type, and  $c$  is its bond coordination number. Bonds are represented by vectors between neighboring lattice sites. Vector orientation is given by a code number  $d$  assuming values from 1 to 12 which describe the 12 possible orientations of the site–site vectors in the 12 coordinated fcc lattice, as illustrated in Figure 3.  $d = 13$  is used as a code for a the vector of length equal to 0. In the cases when single molecules are considered, no spatial limits are assumed. The sizes of molecules are only limited by memory limits of the computer or by time limits of the computation. Motion of simulated molecules allows to generate a large number of states which can be averaged to get representative information about the structure of the molecule in equilibrium. Monitoring displacements of the model molecule and its elements in time, it is possible to get information about the dynamics. Time has been defined here as a number of attempted moves per single bead.

The following model systems (illustrated in Scheme 1) are considered in this paper: (1) linear chains with lengths  $N = 10, 20, 40, 80, 160, 320$ , and 640, (2) simple cyclic chains with nearly the same lengths as in the case of linear chains, and (3) linear catenanes consisting of  $n$  rings with ring lengths  $N_r$  resulting in the total size  $N = nN_r$ , covering the size range of linear chains. The parameters of all simulated systems are given in Tables 1 and 2.

**Scheme 1. Illustration of Polymer Structures Considered in This Paper****Table 1. Lengths of Simulated Linear and Cyclic Chains**

chain type	chain length ( $N$ )						
linear	10	20	40	80	160	320	640
cyclic	10	22	42	82	162	322	642

**Table 2. Sizes ( $N$ ) of Simulated Catenanes for Various Combinations of Parameters  $n$  and  $N$** 

$n$	$N$					
	$N_r = 10$	$N_r = 22$	$N_r = 42$	$N_r = 82$	$N_r = 162$	$N_r = 322$
2	20	44	84	164	324	644
4	40	88	168	328	648	
8	80	176	336	656		
16	160	352	672			
32	320	704				
64	640					

Static properties of the simulated molecules are characterized by various typically used quantities which describe the global size: (i) the mean-square end-to-end distance

$$\langle R^2 \rangle = \langle (r_1 - r_N)^2 \rangle \quad (1)$$

(ii) the mean-square radius of gyration

$$\langle s^2 \rangle = \langle (r_i - r_{cm})^2 \rangle \quad (2)$$

where  $r_1$  and  $r_N$  are space coordinates of chain ends and  $r_i$  and  $r_{cm}$  are space coordinates of monomers and centers of mass of chains, respectively. For cyclic molecules or cyclic elements in catenanes only the radius of gyration is used.

Internal structure of model macromolecules will be described by the site-site correlation function of sites separated by  $r = r_i - r_j$

$$g(r) = \frac{1}{n_p N} \langle c_k(r_i) \cdot c_l(r_j) \rangle \quad (3)$$

where  $c_k$  and  $c_l$  are contrast operators assuming values of 1 for sites occupied by molecular elements and assume 0 at all other sites and  $n_p$  is the number of chains considered, and by the static form factor

$$P(q) = \sum_{ij} g(r) \frac{\sin(qr)}{qr} \quad (4)$$

where  $q$  is the scattering vector. The form factor is determined in order to show which effects can be expected for various macromolecules when studied by scattering methods. The structure of catenanes is also described by means of the mean-square distance between centers of mass of neighboring rings  $\langle R_{rr}^2 \rangle$ . Centers of mass of the first and the last ring in the linear catenane are considered as ends of the whole macromolecule.

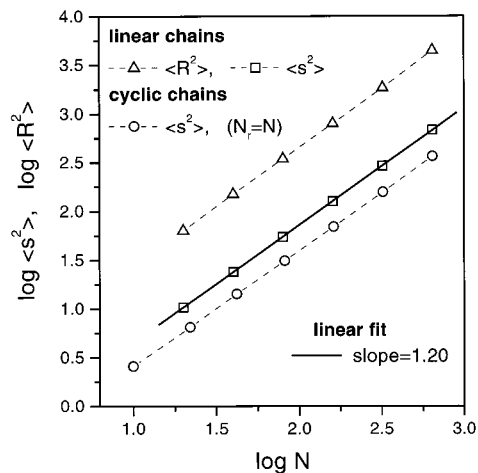


**Figure 4.** Mean sizes of single linear and cyclic chains as a function of chain length. The solid line shows the linear fit indicating the scaling  $\langle s^2 \rangle \propto N^{2\nu}$  with  $\nu = 0.6$ , characteristic for polymers in a good solvent.

The dynamic properties are characterized by auto-correlation functions of bonds and end-to-end vectors

$$\rho_b(t) = \frac{1}{Nn} \sum_n \sum_i b_i(t) \cdot b_i(0) \quad (5)$$

$$\rho_R(t) = \frac{1}{n} \sum_n R(0) \cdot R(t) \quad (6)$$

where  $b_i$  are unit vectors representing bond orientation and  $R$  are end-to-end vectors at time  $t = 0$  and  $t$ . For cyclic molecules of length  $N$  and for rings of length  $N_r$  in catenanes instead of the end-to-end vector, the diametric vector connecting elements separated by  $N/2$  or  $N_r/2$  elements, respectively, has been considered. The relaxation of topological bonds in catenanes is characterized by the time correlation of the ring-ring vector  $R_{rr}$  connecting centers of mass of neighboring rings.

Translation of model elements in space is characterized by the mean square displacements of both beads and the center-of-mass of the whole macromolecule

$$\langle r_m^2 \rangle = \frac{1}{Nn} \sum_n \sum_N [r_m(t) - r_m(0)]^2 \quad (7)$$

$$\langle r_{cm}^2 \rangle = \frac{1}{n} \sum_n [r_{cm}(t) - r_{cm}(0)]^2 \quad (8)$$

where  $r_m(t)$  and  $r_{cm}(t)$  are monomer and chain center-of-mass coordinates at time  $t$ , respectively. In the case of catenanes, translations of individual rings are monitored, as well, by means of the mean-square displacements of their centers of mass.

## Results

**Structure.** Single linear and cyclic chains simulated by the above-described method are used as reference systems for more complex molecules. Mean sizes of the linear and cyclic chains are shown in Figure 4 as a function of chain length. The three dependencies determined indicate a power law scaling of spatial molecular sizes with the length of chains (e.g.,  $\langle s^2 \rangle \propto N^{2\nu}$ ). For all the dependencies, the same scaling exponent  $\nu = 0.6 \pm 0.01$  has been determined, which is characteristic for

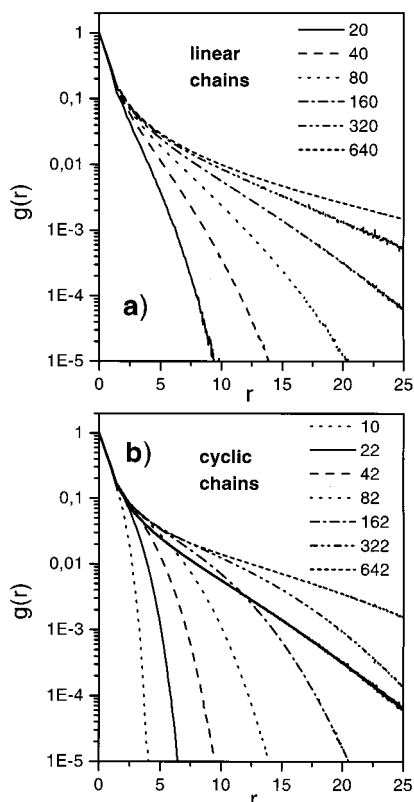


**Figure 5.** Bead–bead correlation functions for linear (a) and cyclic (b) chains of various length. The thick solid line in (b) is replotted from (a) and shows the correlation function for the linear chain of length  $N = 160$  in order to allow a direct comparison with the correlation function for cyclic chain with the corresponding length ( $N = 162$ ).

the behavior of polymers in a good solvent where the conformation is controlled by the excluded-volume interactions. The dimensions of rings, when represented by the mean-square radius of gyration, are approximately 2 times smaller than these of linear chains. It means that the elements of rings occupy a smaller space than the same number of elements forming a linear chain. Rings can, therefore, be considered as more compact molecular objects with higher density of chain segments than in linear chains. This difference is well seen in the site–site correlation functions shown in Figure 5. The correlation function for linear chains with  $N = 160$  is plotted also in Figure 5b in order to allow a direct comparison with the corresponding correlation function for cyclic chains with  $N = 162$ . Higher values of  $g(r)$  at small  $r$  and a smaller range of correlation for cyclic chains is clearly seen. The form factors of both types of macromolecules are shown in Figure 6. The excluded-volume effect in both types of chains is seen in Figure 6a,b as a deviation from the slope of  $-2$  (characteristic for phantom chains) in the intermediate  $q$  range. The difference between the two types of chains is mainly within the small  $q$  range and is illustrated in Figure 6c in the form of the Kratky plot in which the characteristic maximum for cyclic chains is seen.<sup>18</sup>

Catenanes consisting of linear assemblies of identical rings have dimensions smaller than both above types of polymers. An example of mean sizes of catenanes characterized both by the end-to-end distance and by the radius of gyration as a function of the total number of beads is shown in Figure 7a, in comparison with corresponding dependencies for the simple linear and

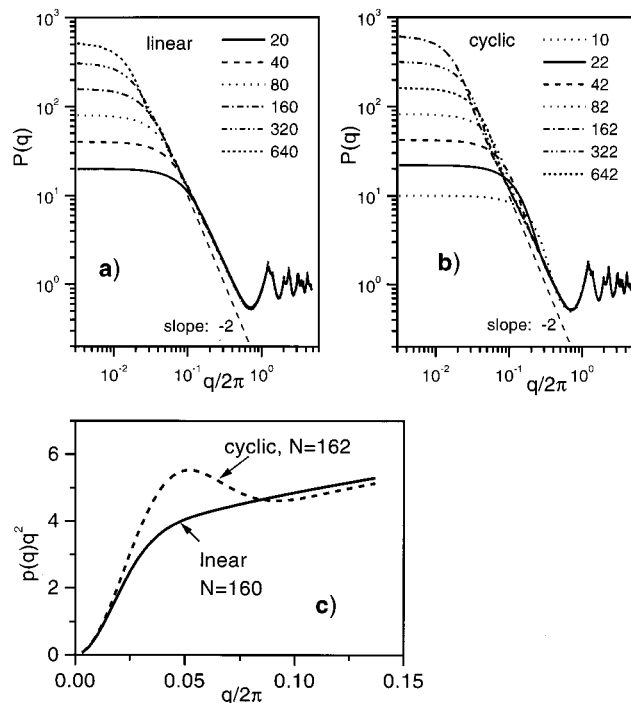


**Figure 6.** Form factors of linear (a) and cyclic (b) chains of various length. The dotted lines show a slope  $-2$  characteristic for the form factors of phantom chains within the intermediate  $q$  range. In (c) the form factors of linear and cyclic chains of nearly the same length are compared in the form of Kratky plots (low  $q$  range).

cyclic chains. The separation between centers of mass of the first and last ring in the assembly is assumed as the end-to-end distance of catenanes. For two concatenated rings the separation of their centers of mass is comparable with the radius of gyration of the whole object. With increasing number of rings values of the two quantities become different assuming, however, for a large number of rings nearly a constant ratio similar to the ratio  $\langle R^2 \rangle / \langle s^2 \rangle$  observed for linear chains. For large  $N$  the dimensions of catenanes tend to approach the same scaling dependencies as has been observed for both linear and ring polymers. For catenanes with a large number of rings the mean sizes of individual rings and the mean distances between them become constant, as seen in Figure 7b. In this limit also the persistence length of catenanes levels off and assumes the value of about 2 when expressed by means of the number of rings about 2 when expressed by means of the number of rings about the catenane. The example shown in Figure 7 concerns catenanes consisting of rings of one size,  $N_r = 10$ . Results characterizing global dimensions of catenanes with various numbers of rings and various ring sizes are shown in Figure 8a. We have noticed that these sizes, when normalized by sizes of individual rings ( $\sim N_r^{1,2}$ ), constitute a master dependence, shown in Figure 8b. This indicates that catenanes with a sufficient number of rings ( $n > 10$ ) can be considered as ordinary linear chains consisting of “macromonomers” in the form of molecular cycles. This allows predictions of catenane sizes for  $n > 10$

$$\langle R^2 \rangle \propto a^2 (nN_r)^{2\nu} \quad (9)$$

In spite of the similarities of size scaling of chains of various kinds, the distributions of chain segments within their correlation range differ considerably. This is illustrated in Figure 9 by a comparison of the site–

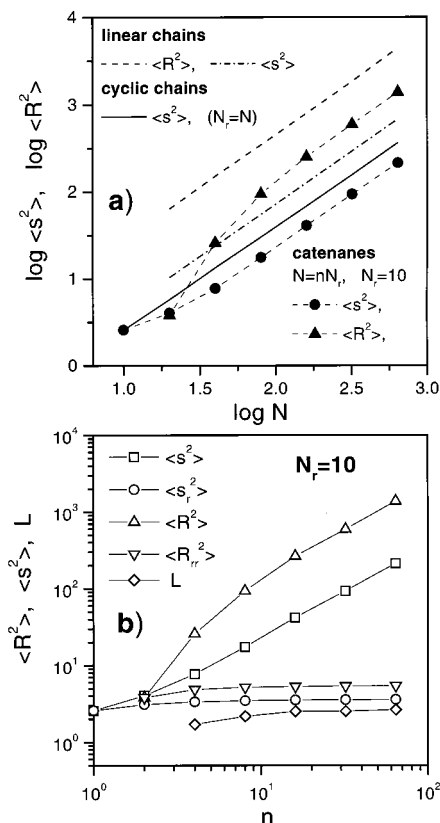


**Figure 7.** (a) Sizes of catenanes with various numbers of rings of length  $N_r = 10$  characterized by means of the mean-square radius of gyration and the mean-square end-to-end distance. For comparison, dependencies for linear and cyclic chains (as in Figure 4) are shown. (b) The total radius of gyration  $\langle s^2 \rangle$ , the end-to-end distance  $\langle R^2 \rangle$ , the radius of gyration of single ring  $\langle s_r^2 \rangle$ , the ring–ring separation  $\langle R_r^2 \rangle$ , and the persistence length  $L$  of catenanes with  $N_r = 10$  as a function of the number of rings.

site correlation functions for polymers with nearly the same total number of beads but different architecture of the macromolecule. For catenanes, a higher local space filling and consequently smaller sizes in comparison with linear or cyclic chains are observed. The form factors for the different types of polymers are shown in Figure 10, in the two representations: first (Figure 10a) presenting the behavior in a broad  $q$  range and the second (Figure 10b) indicating distinct differences between different types of macromolecules within the low  $q$  range, in spite of almost identical numbers of segments within macromolecules considered. An illustration of conformations of some molecular structures differing by the type of arrangement of chain segments but nearly with the same number of segments is shown in Figure 11.

**Elasticity.** Elastic properties of polymers assuming statistical conformations can be characterized by means of the force–extension relation which can be determined on the basis of the probabilities to assume conformations with a particular separation of given chain elements, e.g., chain ends, which are considered as points where the forces are applied.<sup>19</sup> For the chains simulated in this paper the following elements are distinguished for such considerations: (1) chain ends, in the case of linear chains, (2) beads separated by  $N_r/2$  along the ring contour, in the case of simple cyclic chains, and (3) arbitrary selected beads in the first and last ring of the catenane. Probability distributions to assume conforma-

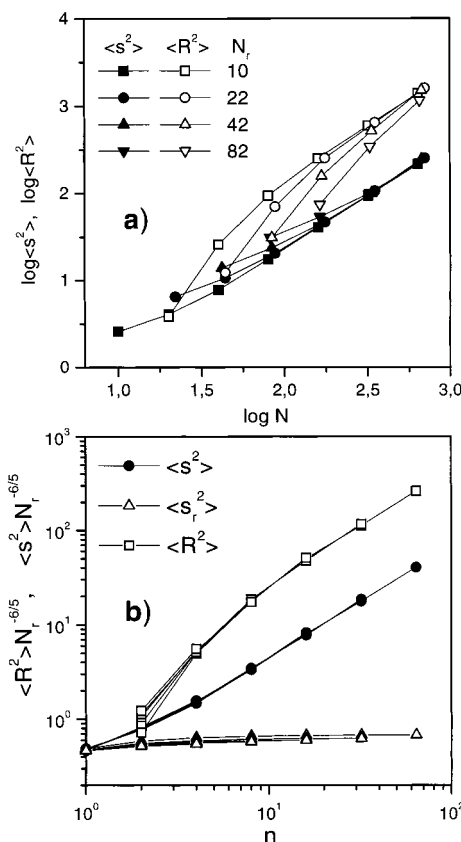


**Figure 8.** (a) Sizes of catenanes with various numbers of rings and various ring lengths as a function of the total number of beads. (b) The same quantities normalized by ring size, presented as a function of ring number.

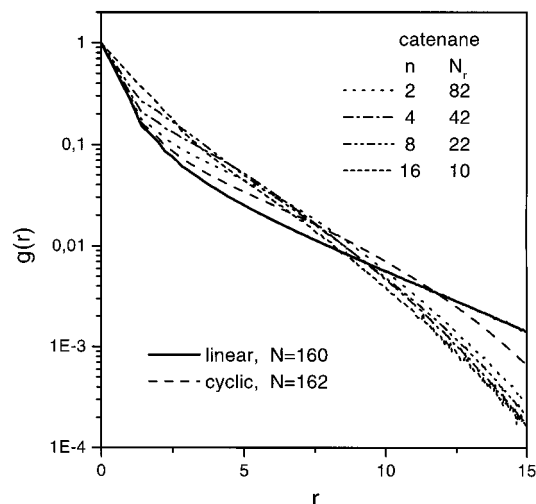


**Figure 9.** Bead–bead correlation functions for catenanes with approximately the same total number of beads distributed in various number of rings of different lengths. For comparison, the correlation functions for linear and cyclic chains are shown.

tions with various separations of these elements have been determined and are shown in Figure 12 for model systems with approximately the same number of monomers which, however, are organized to macromolecules with various architectures. Both the positions of the most probable separations and the widths of the distributions differ for various systems, suggesting differences in elastic properties of various chains.

A tensile force which can cause a change in the distance  $r$ , between the distinguished elements, to a

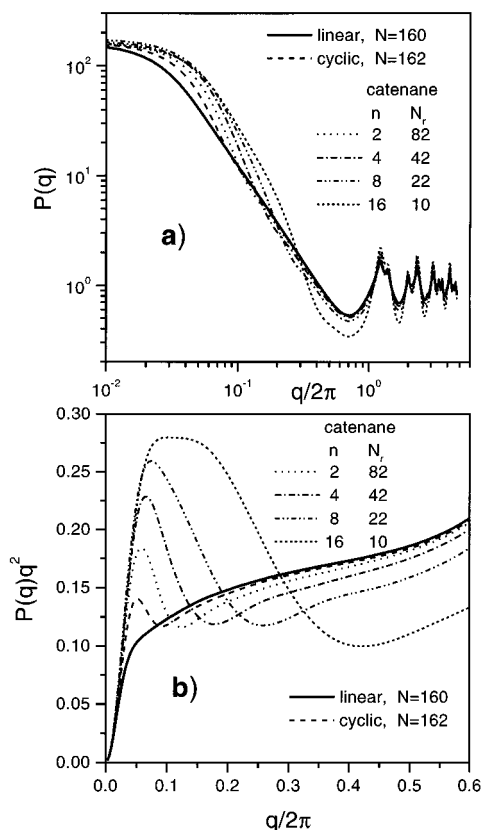


**Figure 10.** Form factors of catenanes with approximately the same total number of beads but different ring lengths. Both the log–log representation in a broad  $q$  range and a Kratky representation for the low  $q$  range are shown in (a) and (b), respectively.

distance  $r + dr$  corresponds to the work ( $dW = f dr$ ), which has to be done. The latter is given by the change of Helmholtz free energy ( $dF$ ) and corresponding change of entropy ( $dS$ ):

$$dW = dF = -T dS \quad (10)$$

The entropy can be related to the distribution of probabilities of conformational states  $p(r)$  as follows:

$$S \propto k \ln p(r) \quad (11)$$

where  $k$  is the Boltzmann constant. Considering this, we obtain a relation between forces and distances for the distinguished chain elements

$$\frac{f}{kT} \propto - \frac{d(\ln p(r))}{dr} \quad (12)$$

This relation can be numerically determined on the basis of the probability distributions  $p(r)$  obtained for the simulated molecules. Results for the range of small deformations are presented in Figure 13. The deformation of chains is characterized by the draw ratio  $\lambda = r/r_{\max}$ , where  $r_{\max}$  is the most probable separation of chain ends. The limitation in determination of such dependencies for large deformations are caused by limits in accuracy with which the distributions  $p(r)$  can be determined for states corresponding to large fluctuations of chains from the most probable conformations. The results in Figure 13 indicate almost linear force–deformation dependencies within the considered deformation range. Properties of chains of various kinds can

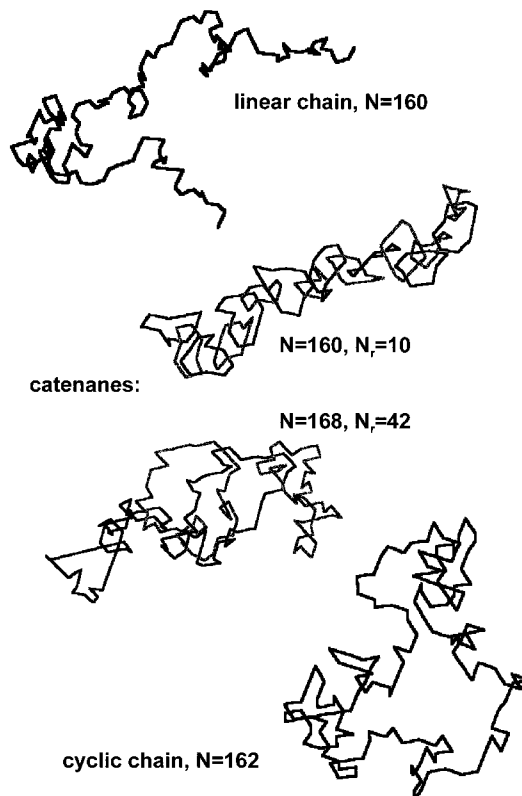


**Figure 11.** Illustration of conformations of some catenanes in comparison with linear and cyclic chains of similar total length.

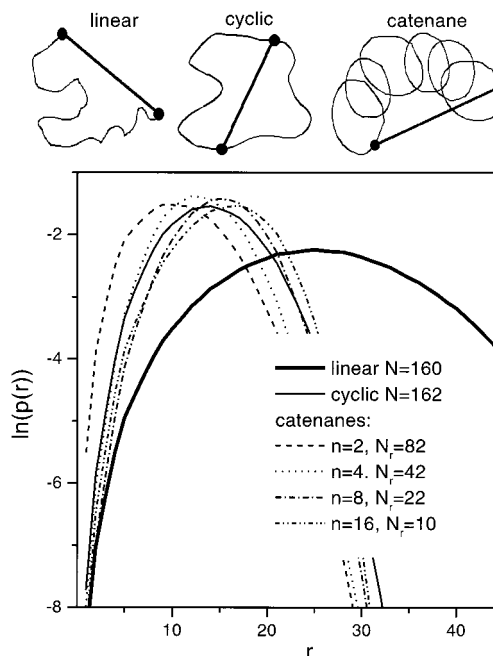


**Figure 12.** Distributions of end-to-end distances in linear chain, diagonal distances in cyclic chain, and distances between two beads located in opposite end rings of various catenanes. The distances considered are illustrated in the upper part of the figure.

be characterized by the tensile modulus ( $E \propto f(\lambda - 1)$ ) which is given by the slope in the force–deformation relation. When various kinds of chains with a nearly the same number of monomers are compared, the smallest modulus is observed for linear chains; it increases for the cyclic polymers by approximately a

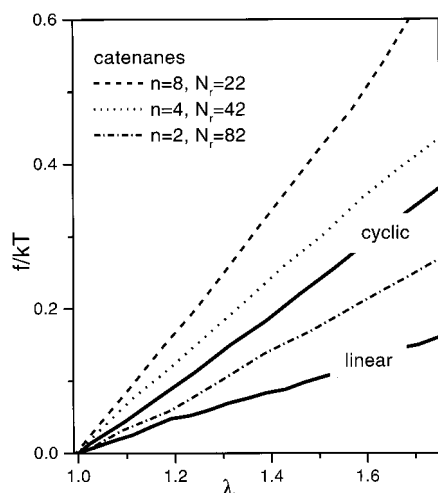


**Figure 13.** Force–deformation relations for various catenanes (small deformation range), in comparison with cyclic and linear chains of corresponding total length. The tension is applied to the characteristic points illustrated in the upper part of Figure 12.

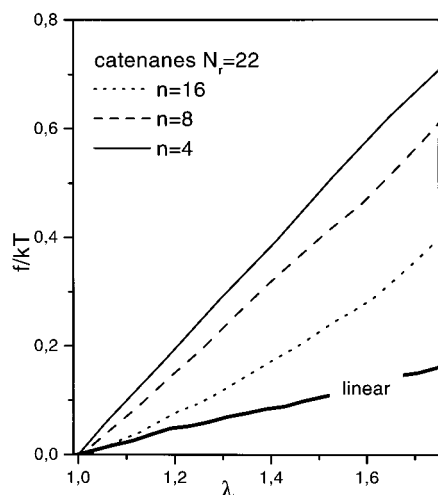


**Figure 14.** Effect of the number of rings in catenanes on the force–deformation dependencies (small deformation range).

factor of 2 and increases further for catenanes with increasing number of rings when the total number of monomers is kept constant. The effect of ring number in catenanes with the ring length kept constant is illustrated in Figure 14. This result indicates that for a larger number of rings the modulus drops toward the value one can observe for a simple linear molecule with the contour length corresponding to the total backbone length in the catenane.

**Dynamics.** An example of the dynamic behavior of linear chains, as observed in the simulation, is shown in Figure 15. Bond and end-to-end autocorrelation functions for chains of various lengths are shown in Figure 15a, and the mean-square displacements of beads and chain centers of mass are in Figure 15b. The dependencies are determined as averages of more than 500 runs for individual molecules starting from independent initial states. The correlation functions of bonds and end-to-end vectors of chains are used for determination of corresponding relaxation times by fitting of the stretched exponential functions. In the case of cyclic chains the relaxation times of whole molecules have been determined from the autocorrelation functions of the diametric vectors (connecting segments separated

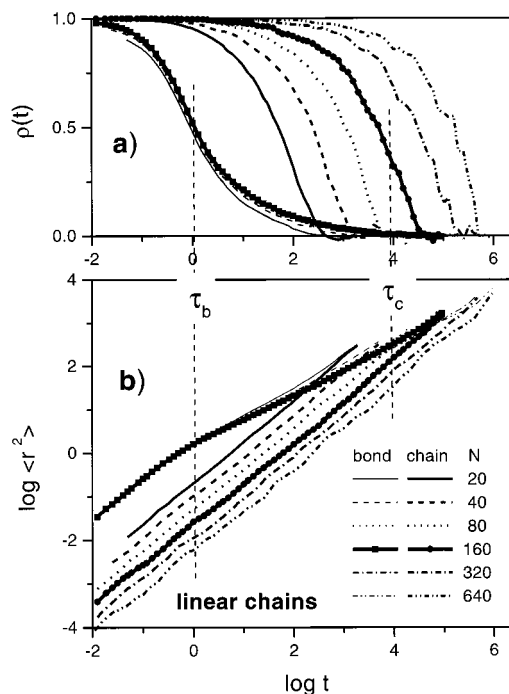


**Figure 15.** Dynamic properties of linear chains of various lengths characterized by the autocorrelation functions of bonds and end-to-end vectors (a) and by the mean-square displacements of beads and centers of mass of chains (b). The vertical dashed lines indicate the relaxation times of bonds ( $\tau_b$ ) and whole chains ( $\tau_c$ ) for chains of length  $N = 160$ .

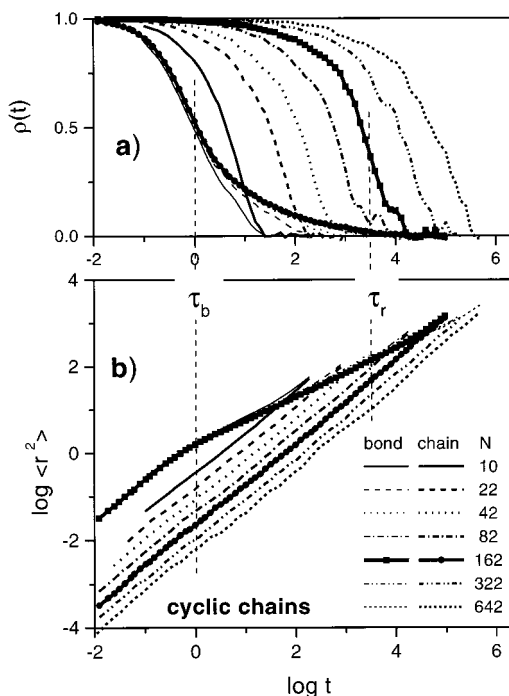


**Figure 16.** Dynamic properties of cyclic chains of various lengths characterized by the autocorrelation functions of bonds and diametric vectors (a) and by the mean-square displacements of beads and of the centers of mass (b). The vertical dashed lines indicate the relaxation times of bonds ( $\tau_b$ ) and whole chains ( $\tau_r$ ) for chains of length  $N = 162$ .

by  $N_r/2$  along the chain contour) as shown in Figure 16. Diffusion constants of chains have been determined from the mean-square displacements of the centers of mass at the long time limit. Chain length dependencies of these quantities both for linear and cyclic chains are

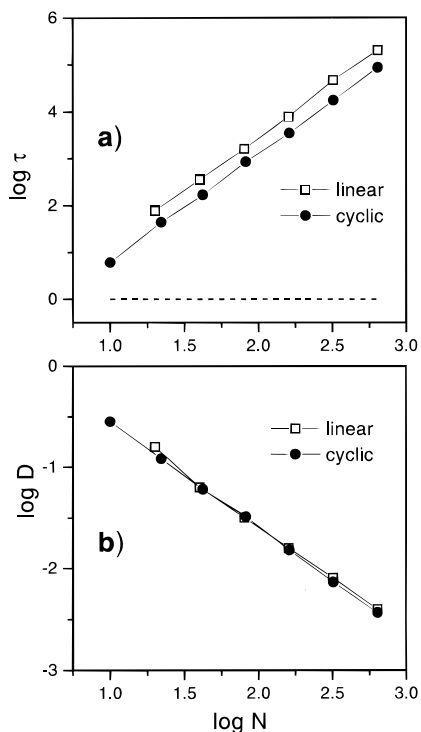


**Figure 17.** Chain length dependencies of the relaxation times (a) of end-to-end vectors of linear chains and diametric vectors of cyclic chains and the chain length dependencies of the diffusion constants (b) of these two kinds of chains. The dashed line in (a) represents relaxation times of bonds in both linear and cyclic chains.

shown in Figure 17. They indicate that the diffusion constants of the two kinds of chains do not differ remarkably ( $\langle D_{\text{lin}}/D_{\text{cyc}} \rangle = 1.06$ ) and have the same chain length dependence which can be characterized by a scaling power law  $D \propto N^\alpha$  with  $\alpha = -1.04 \pm 0.02$ . The segmental relaxation rates in both kinds of chains remain at short times independent of chain length and do not differ for the two kinds of chains. The relaxation times of end-to-end vectors of linear chains, characterizing mainly their orientational relaxation, are by a factor of 2.2 (in average) longer than the relaxation times describing reorientation of the diametric vectors in cyclic chains of corresponding length. Both, however, scale with the chain length ( $\tau \propto N^\beta$ ) with the same exponent  $\beta = 2.28 \pm 0.03$ .

The dynamics of catenanes having more complex structure than linear and cyclic chains is characterized by a number of correlation functions corresponding to relaxation of various structural elements. This included single bonds, the diametric vectors of individual rings ( $R_r$ ), the center-to-center vectors of neighboring concatenated rings ( $R_{rr}$ ), and the end-to-end vectors ( $R_c$ ) of the whole catenane. The vectors are illustrated schematically in Figure 18. Mean-square displacements have been monitored in time for beads, for centers of mass of individual rings, and for the centers of mass of whole macromolecules. Results for a series of catenanes with various numbers of rings of the same length ( $N_r = 10$ ) are shown in Figure 19. The relaxation times of the different structural elements of the catenane with 16 rings are marked in the figure by vertical dashed lines. They are distinctly separated each from the other and strongly related to catenane parameters: ring length and ring number. Generally catenanes as a whole appear slower than linear or cyclic chains of correspond-

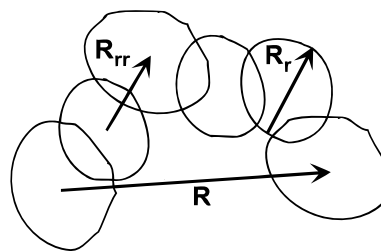


**Figure 18.** Illustration of characteristic vectors for which the relaxation has been detected:  $R_r$  = the diametric vector of a ring,  $R_{rr}$  = the topological bond vector connecting centers of mass of neighboring rings, and  $R_c$  = the end-to-end vector of the catenane.

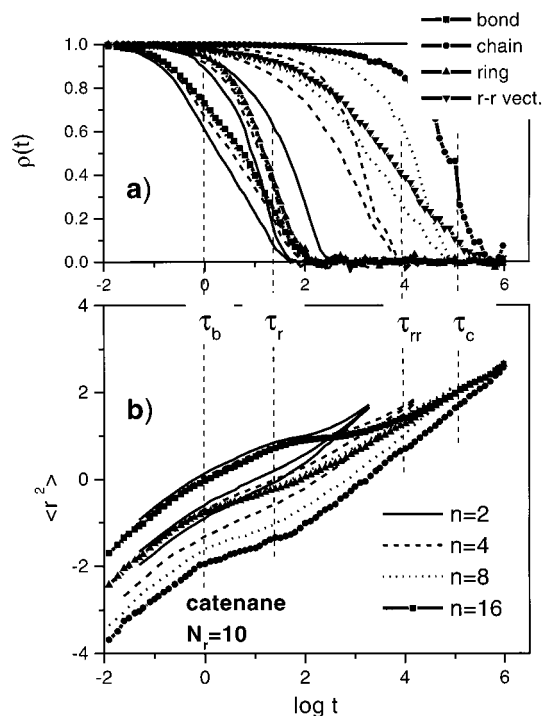


**Figure 19.** Dynamic properties of catenanes with various numbers of rings ( $n = 4, 8,$  and  $16$ ) and constant ring length  $N_r = 10$ : (a) the autocorrelation functions of bonds, of ring diametric vectors ( $R_r$ ), of ring–ring vectors ( $R_{rr}$ ), and of the end-to-end vectors ( $R_c$ ); (b) the mean-square displacements of beads, of the centers-of-mass of rings, and of the centers-of-mass of catenanes. The vertical dashed lines indicate the relaxation times of bonds ( $\tau_b$ ), of rings ( $\tau_r$ ), of ring–ring vectors ( $\tau_{rr}$ ), and of the whole catenanes ( $\tau_c$ ), for the system with 16 rings ( $N = 160$ ).

ing chain length ( $N$ ). For catenanes with large flexible rings, however, the slowing down is rather small. The slowing down is mainly related to the large separation between relaxation times related to rotation of individual rings and these related to relaxation of the topological bonds between the neighboring rings. It appears large for short rings, as illustrated in Figure 19. This effect is also well seen in the displacements of beads constituting catenanes. There is a specific sequence of slopes in time dependencies of bead displacements which is quite different from that observed for linear or cyclic chains. For simple chains the displacements of beads can be approximated by a sequence of power laws  $t^\gamma$  with the exponents  $\gamma = 1, 0.5,$  and  $1$ , which characterize the short time bead mobility, the non-Fickian diffusion during the chain relaxation, and the long time diffusion of whole molecules, respectively. For catenanes, the intermediate range related ap-

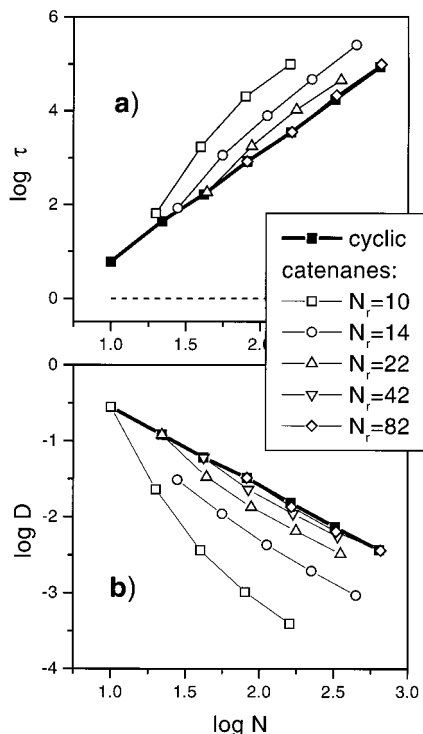


**Figure 20.** Chain length dependencies of the relaxation times of end-to-end vectors (a) and of the diffusion constants (b) for catenanes with various numbers of rings and various ring sizes, in comparison with corresponding dependencies for cyclic chains. The dashed line in (a) represents relaxation times of cyclic bonds.

proximately to the time period of chain relaxation is broken into three subranges with exponents  $\gamma = 0.5$ ,  $\gamma_p$ , and  $0.5$  where  $\gamma_p$  slightly depends on the number of rings and assumes values close to 0, as indicated by the almost horizontal plateau observed for catenanes with the number of rings,  $n = 16$ . This to some extent resembles the dynamics of linear chains in entangled melts<sup>20</sup> where, however, the exponent  $\gamma_p$  is not smaller than 0.25. Such behavior of catenanes shows a complexity of their dynamics which can be strongly influenced by playing with the two structure parameters: the size and the number of rings. The total slowing down of catenanes with respect to cyclic chains is characterized in Figure 20, by means of the relaxation times of end-to-end vectors and diffusion constants. It is seen that increasing the number of rings in catenanes, when the total number of monomers is kept constant, which is equivalent to a replacement of chemical bonds by the topological bonds, leads to considerable slowing down of the molecules. For constant ring length, however, and a sufficiently large number of rings ( $n > 10$ ), the chain length dependencies of both the relaxation times and the diffusion constants for catenanes become similar to these of simple linear or cyclic chains and can be characterized by power laws with similar exponents. The slowing down of catenanes with the large number of rings reflects only in the prefactors of corresponding scaling laws. The change of the global dynamics with respect to cyclic chains is only considerable for catenanes consisting of short rings. As the results in Figure 20 show, for catenanes consisting of rings with  $N_r = 82$ , both the relaxation times and the diffusion constants are indistinguishable from these of cyclic chains of corresponding length.

## Conclusions

We have presented here a comprehensive characterization of properties of single linear catenanes in states corresponding to macromolecules in a good solvent. The results are based on simulations using the cooperative motion algorithm. Behavior of catenanes has been compared with the behavior of linear and simple cyclic chains considered under the same conditions.

It has been shown that spatial dimensions of catenanes with a sufficient number of rings can be characterized in the same way as for linear chains, i.e., by means of scaling laws with exponents characteristic for polymers with strong excluded-volume interactions. Additionally, catenane dimensions can be represented by a master dependence on the number of rings when the sizes of whole molecules are normalized by sizes of individual rings. Catenanes constitute generally more compact molecules than the linear or cyclic chains with the same number of monomers. Particle factors of catenanes with various parameters are presented.

Elastic properties of catenanes have been characterized by means of an analysis of distributions of their end-to-end sizes. It has been shown that their tensile modulus at small deformations can exceed the elastic constants of both simple linear and cyclic chains and can be varied in a rather broad range by changing the ring size and the number of rings.

Higher complexity of the architecture of catenanes in comparison with linear or cyclic chains makes the dynamics of such molecules much more complex. For catenanes consisting of short rings, a large separation of relaxation times corresponding to local mobility of individual rings and those corresponding to relaxation of the topological bonds between neighboring concatenated rings leads to a distinct plateau in monomer displacements and causes a considerable slowing down of relaxation of whole molecules with respect to relaxation rates of linear or cyclic chains with corresponding numbers of monomers. The slowing down increases with the increase of number of rings to which a given number of monomers is distributed. On the other hand, for a constant number of rings, interactions between neighboring rings become weaker with increasing ring size  $N_r$ , so that large concatenated rings can be considered as almost independent. This reflects in nondistorted sizes of such rings within catenanes and in diffusion and relaxation rates of catenanes dependent only on the total number of segments.

The results, however, limited to single molecules have shown that catenanes exhibit some specific properties that cannot be found in either linear or cyclic polymer chains. This concerns mainly their dynamics which for single catenanes can become as complex as for other polymers in dense systems.

We have considered here linear catenanes as the simplest example of topologically interacting rings. The same methods can, however, be applied to a number of other related problems such as the problem of conformation of multiple linked DNA rings studied recently both experimentally<sup>21</sup> and theoretically.<sup>22,23</sup>

**Acknowledgment.** We acknowledge M. Benmouna and T. A. Vilgis for helpful comments. This work was partially supported by the KBN Project No. 3T09A04314 (Poland).

## References and Notes

- (1) Ambilino, D. B.; Stoddart, J. F. *Chem. Rev.* **1995**, *95*, 2725.
- (2) Webster, O. W. *Macromol. Symp.* **1995**, *98*, 1361.
- (3) Grest, G. S.; Kremer, K.; Milner, S. T.; Witten, T. A. *Macromolecules* **1989**, *22*, 1904.
- (4) Pakula, T. *Comput. Theor. Polym. Sci.* **1998**, *8*, 21.
- (5) Pakula, T.; Geyler, S.; Edling, T.; Boese, D. *Rheol. Acta* **1996**, *35*, 631.
- (6) Lue, L.; Prausnitz, J. M. *Macromolecules* **1997**, *30*, 6550.
- (7) Grest, G.; Fetters, L. J.; Huang, J. S.; Richter, D. *Adv. Chem. Phys.* **1996**, *94*, 67.
- (8) Rey, A.; Freire, J. J.; de la Torre, J. G. *Macromolecules* **1987**, *20*, 342.
- (9) Freire, J. J. *Adv. Polym. Sci.* **1999**, *35*, 143.
- (10) Gauger, A.; Pakula, T. *Macromolecules* **1995**, *28*, 190.
- (11) Pitsikalis, M.; Hadjichristidis, N. *Macromolecules* **1995**, *28*, 3904.
- (12) Pakula, T.; Matyjaszewski, K. *Macromol. Theory. Simul.* **1996**, *5*, 987.
- (13) Pakula, T. *Macromolecules* **1987**, *20*, 679. Pakula, T.; Geyler, S. *Macromolecules* **1987**, *20*, 2909. Pakula, T. *Recent Res. Dev. Polym. Sci.* **1996**, *1*, 101.
- (14) Huff, J.; Preece, J. A.; Stoddart, J. F. *Macromol. Symp.* **1996**, *102*, 1.
- (15) Muscat, D.; Witte, A.; Köhler, W.; Müllen, K.; Geerts, Y. *Macromol. Rapid Commun.* **1997**, *18*, 238.
- (16) Vogtle, F.; Jager, R.; Handel, M.; Ottenshildebrandt, S. *Pure Appl. Chem.* **1996**, *68*, 225.
- (17) Yamamoto, C.; Okamoto, Y.; Schmidt, T.; Jager, R.; Vogtle, F. *J. Am. Chem. Soc.* **1997**, *119*, 10547.
- (18) Geyler, S.; Pakula, T. *Makromol. Chem. Rapid Commun.* **1988**, *9*, 617.
- (19) Treloar, L. R. G. In *The Physics of Rubber Elasticity*; Clarendon Press: Oxford, 1975; Chapter 3.
- (20) Doi, M.; Edwards, S. F. In *The Theory of Polymer Dynamics*; Clarendon Press: Oxford, 1988.
- (21) Levene, S. D.; Donahue, C.; Boles, T. C.; Cozzarelli, N. R. *Biophys. J.* **1995**, *69*, 1036.
- (22) Otto, M.; Vilgis, T. A. *Phys. Rev. Lett.* **1998**, *80*, 881.
- (23) Wei, G. *Polym. Adv. Technol.* **1997**, *8*, 265.

MA990248C